Impact of bentonite colloids on radionuclide transport in fractured systems – results from field experiments and modeling

Ulrich Noseck, Judith Flügge*, Thorsten Schäfer**,§*

*Gesellschaft für Anlagen- und Reaktorsicherheit (GRS) mbH / Theodor-Heuss-Str. 4, 38122 Braunschweig, Germany

** Karlsruhe Institute of Technology, Institute for Nuclear Waste Disposal (INE) / P.O. Box 3640, 76021 Karlsruhe, Germany

§Institute of Geological Sciences, Department of Earth Sciences, Freie Universität Berlin, 14195 Berlin, Germany

Abstract: 2D flow and transport calculations are performed to describe field dipole experiments with FEBEX bentonite colloids and lanthanides (as homologues for tri- and tetravalent actinides). The experiments are undertaken at different flow velocities in a shear zone at the Grimsel Test Site within the international Colloid Formation and Migration (CFM) project. After calibration of the flow model using the uranine breakthrough curve of one dipole experiment the model is successfully applied to other dipole experiments conducted at different flow velocities. The simulation of the colloid-facilitated transport is performed for two experiments with different flow velocities. The results show, that the interaction of the colloids with the fracture filling material can be reasonably well described by one set of parameters considering a reversible and an irreversible attachment process. The breakthrough curve of the lanthanides as well as their mass recovery is controlled by the desorption kinetics from the colloids. The desorption rates obtained from the field experiment at longer residence time agree well with results from independent batch experiments. The observed decrease of the desorption rate with travel time is not yet clarified and will be investigated further in future dipole experiments to be carried out in the shear zone.

1 INTRODUCTION

Long-term safety assessments of repositories for radioactive waste require a comprehensive system understanding and a programme package to simulate the relevant processes expected in the future evolution of the repository system. An important part of the repository system is the geological barrier, which is – in case of disposal concepts for hard rock – presented by the granite host formation. One process to be addressed in long-term safety assessment for these concepts is the colloid-facilitated radionuclide transport through the water conducting features (WCF) in the granitic host rock, which might lead to an increase of radiation exposures. It is particularly discussed that at conditions of very low mineralized waters clay colloids are released from the bentonite buffer by erosion processes, e.g. [1], [2], [3], [4]. Such conditions might occur down to the depth, where the repository will be situated, after melting of thick inland ice sheets during or after glacial periods [5].

In order to assess the impact of bentonite colloids on the long-term safety of a repository in granite a series of lab and field experiments at the underground laboratory at Grimsel Test Site (GTS, www.grimsel.com) is performed within the international partner project Colloid Formation and Migration (CFM) under auspices of NAGRA, Switzerland [6]. One cluster of experiments are dipole tests in the shear zone with FEBEX bentonite (Ca-bentonite) colloids and radionuclides or homologues under defined flow conditions, which are similar to those

expected in natural systems and are therewith close to repository-relevant conditions. In order to identify the relevant interaction processes between radionuclides/homologues, colloids and fracture filling material in the shear zone during transport these experiments are accompanied by model simulations, performed by GRS and other organizations. The focus of this paper is on such model simulations applied to the selected dipole experiments CFM RUN 08-02, CFM RUN 10-01, CFM RUN 10-03 and CFM RUN 12-02 (see table 1 for details). In a first step the hydraulic parameters have been fitted for CFM RUN 10-01 and applied to simulate the breakthrough curves of the ideal tracers in the other experiments. In further steps the migration of the colloids and their interaction with the fracture filling material as well as the migration of the homologues and their interactions with colloids and fracture filling material are modeled for the experiments CFM RUN 10-01 and CFM RUN 10-03.

2 DIPOLE EXPERIMENTS

The field tracer tests CFM RUN 08-02, CFM RUN 10-01, CFM RUN 10-03 and CFM RUN 12-02 have been performed within the CFM project in a dipole between the injection interval of borehole CFM 06.002 and the extraction point at Pinkel surface packer as illustrated in Fig. 1. The distance between injection borehole and extraction point (Pinkel) is app. 6.2 m. Details of the experiments can be found in [7].

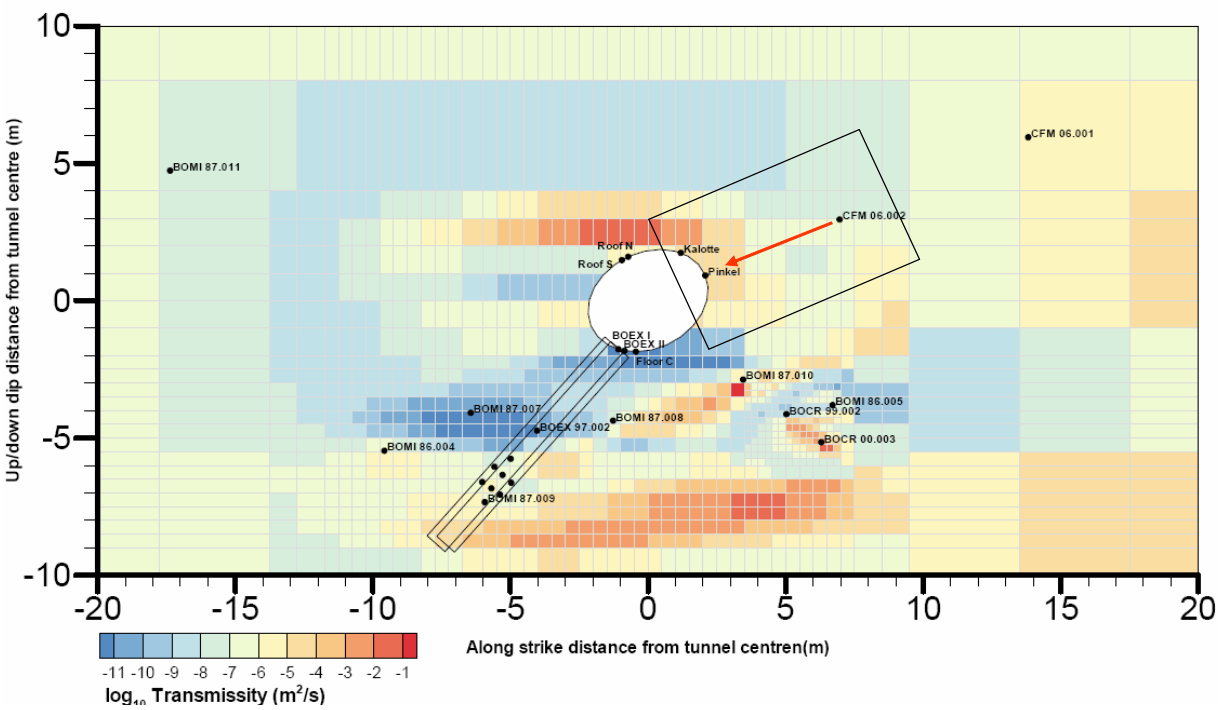

Fig. 1: Transmissivity field and location of boreholes in the shear zone. The dipole between borehole CFM 06.002 and extraction point (Pinkel) for the CFM homologue experiment is indicated by the red arrow (after [8]).

With exception of CFM RUN 08-02 all field tests have been performed as point dilution tests. The transport velocity of the fluid and therewith the residence time of the tracers is mainly determined by the extraction flow rate at the Pinkel, which is varied down to a range approaching the natural conditions within the shear zone. Relevant data for modeling including the injected amounts of the ideal tracer, bentonite colloids and homologue tracers are shown in Tab. 1. Injection functions of all tracers have been monitored and provided for modeling (not shown). For CFM RUN 08-02 and CFM RUN 12-02 only the results of the ideal tracer are evaluated here. For CFM RUN 12-02 bentonite colloids and radionuclide tracers have been applied. The data of the breakthrough curves and recoveries are not available yet but will be provided soon and be used in future modeling work.

For CFM RUN 08-02, CFM RUN 10-01 and CFM RUN 10-03 uranine and for CFM RUN 12-02 Amino G Acid (AGA) have been used as ideal tracers. For CFM RUN 10-03 no reliable uranine breakthrough curve was obtained, which is considered in the simulations, accordingly. The FEBEX bentonite colloids and the homologues have been equilibrated in Grimsel water before injection into the dipole. It was shown that the homologues are nearly quantitatively (between 95% and 100%) bound to the colloids in the injection solution.

Tab. 1: Inflow/outflow conditions, injected amount of tracers and recovery of ideal tracers for the considered field tests. n.c. denotes that these data are not considered for modeling [7]

	CFM RUN 08-02	CFM RUN 10-01	CFM RUN 10-03	CFM RUN 12-02
Inflow [ml/min]	10	-	-	0.33
Outflow [ml/min]	165	48	10	25
Injected amount [mg] of tracers considered for modeling				
Ideal tracer	15.4	5	9	4.5
FEBEX bentonite colloids[1]	n.c.	30	210	n.c.
^{152}Eu		$11.96 \cdot 10^{-3}$	$45.48 \cdot 10^{-3}$	
^{159}Tb		$10.10 \cdot 10^{-3}$	$45.44 \cdot 10^{-3}$	
^{178}Hf		$12.78 \cdot 10^{-3}$	$51.64 \cdot 10^{-3}$	
^{232}Th		$14.87 \cdot 10^{-3}$	$49.78 \cdot 10^{-3}$	
Recovery of the ideal tracer [%]	99	84	90[2]	80

[1] based on Al content measured by ICP-MS
[2] recovery of CFM RUN 10-02, which was performed under same flow conditions as CFM RUN 10-03

3 MODEL AND DATA

Flow and transport calculations have been carried out using the codes d³f [9] for the flow simulations and r³t [10] for the transport simulations. The shear zone of the CFM experiment consists of a network of open channels embedded into fracture infill material and enclosed by quasi-parallel granite walls, whose distance is small compared to their extent. The modeling approach is to simplify the complexity of the fracture network by treating the shear zone as a porous medium with effective flow properties. The typical number of fractures in the shear zone and representative aperture widths are given e.g. in [8]. From these values, a model shear zone thickness of about 5 mm is derived, which is necessary to reduce the imposed boundary conditions to two dimensions.

The flow in the shear zone is determined by the transmissivity field, which is mainly dominated by the external boundary conditions (inflow/outflow) of the dipole. The model size is chosen large enough to reduce wall effects [11]. A scheme of the conceptual model, with initial and boundary conditions adapted for the tracer tests CFM RUN 08-02, CFM RUN 10-01, CFM RUN 10-03 and CFM RUN 12-02 is shown in Fig. 2.

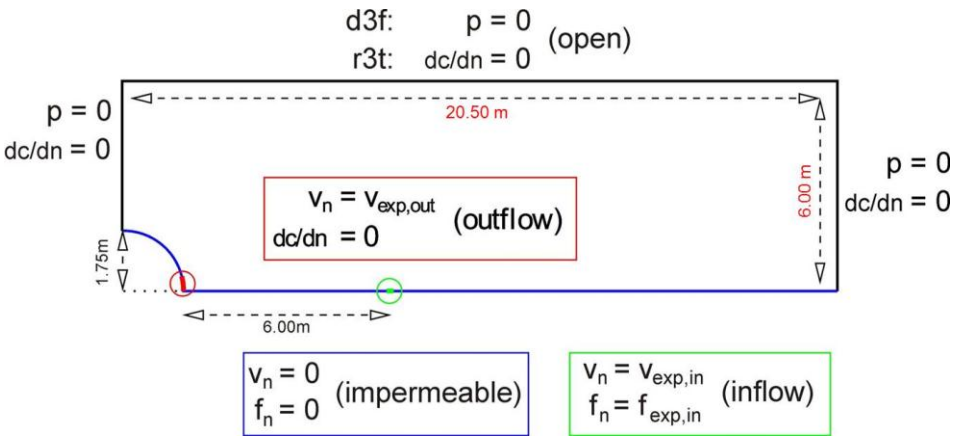

Fig. 2: Geometry and hydrogeological/transport-related boundary conditions of the 2D computer model. Green: Inflow; Red: Outflow; Blue: Sealed tunnel wall and symmetry axis; Black: Permeable virtual boundaries within the shear zone. Notation: c = concentration; p = pressure; v = fluid velocity; f = pollutant mass flux; n is used either as a subscript to denote the normal component or in fractions in which n symbolizes the normal derivative of the respective variable

The conceptual and mathematical model for transport of colloids and pollutants as well as the interaction processes is described in detail in [12]. Fig. 3 illustrates the denotation of the different interaction processes. The sorption process of the free pollutant on the fracture filling material is described by the rate k_1. The sorption process of the free pollutant on mobile and immobile colloids is described by the rates k_3 and k_4, respectively. The interaction process of the colloids with the fracture filling material is described by the rates K_2 and k_2.

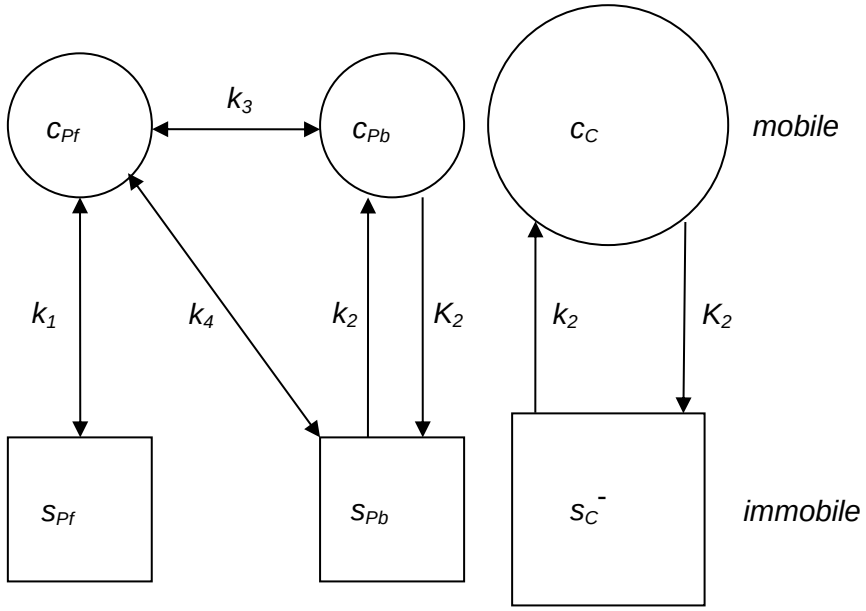

Fig. 3: Denotation for the concentrations of the pollutant and the colloid as well as for the sorption reactions. For more explanations see text

The mass exchange between the above mentioned phases is governed by the following source terms Q:

$$Q_1^P = k_1 \rho (f_1(c_{Pf}) c_{Pf} - s_{Pf}) \quad \text{(Eq. 1)}$$

$$Q_3^P = k_3 \theta (f_3(c_{Pf}) c_{Pf} - c_{Pb}) \quad \text{(Eq. 2)}$$

$$Q_4^P = k_4 (\rho_C s_C f_4(c_{Pf}) c_{Pf} - s_{Pb}) \quad \text{(Eq. 3)}$$

with concentration of contaminants in the dissolved phase c_{Pf}, concentration of contaminants sorbed to mobile colloids c_{Pb}, concentration of contaminants sorbed to the sediment matrix

S_{Pf}, concentration of contaminants sorbed to immobile colloids S_{Pb}, effective matrix porosity θ, matrix bulk density ρ colloid density ρ_C transition rates k_i and K_i and sorption isotherms f_i. The sorption isotherms f_i can be of linear (K_d) or non-linear (Langmuir or Freundlich) type. For simulation of the homologue experiments in CFM the linear K_d-concept is chosen for all pathways, since the tracer concentrations are low enough to be far below saturation of sorption sites and no inhomogeneities and competition for sorbing sites on the rock matrix and colloid surfaces are considered.

The interaction of colloids with the sediment can be described in r^3t by a first order kinetics according to

$$Q_2^C = K_2\theta\, c_C - k_2\rho_C s_C \qquad \text{(Eq. 4)}$$

with the attachment and detachment rates k_2 and K_2. An irreversible attachment / filtration of colloids can be realized by a detachment rate of zero. Consistent with this formulation the change of the contaminant concentration caused by colloid sediment interactions is

$$Q_2^P = K_2\theta\, c_{Pb} - k_2\, s_{Pb} \qquad \text{(Eq. 5)}$$

.

4 RESULTS AND DISCUSSION

In step 1 the non-sorbing solute tracer breakthrough curve of uranine is fitted for CFM RUN 10-01, which is in the focus of our investigation, by varying the dispersivity and porosity. The normalized breakthrough curves (observed concentrations divided by injection masses) are shown in Fig. 4.

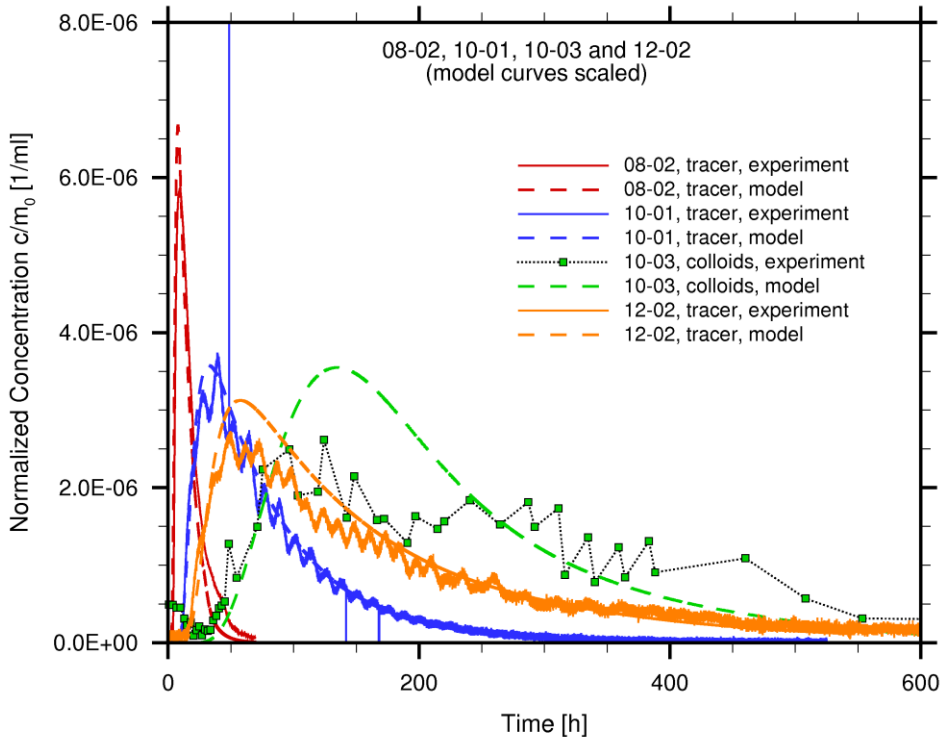

Fig. 4: Ideal tracer breakthrough curves for the dipole experiments CFM RUN 08-02, CFM RUN 10-01, CFM RUN 10-03 and CFM RUN 12-02 (continuous line), and simulated breakthrough curves (dashed line) applying the best-fit hydraulic parameters given in Tab. 1

The flow and transport calculations with the same parameters except inflow/outflow values and injection function, which are different for each run, applied to the breakthrough of the ideal tracers in runs 08-02, and 12-02 show a reasonably well agreement. It should be noted that all results for the CFM RUNs 10-01, 10-03 (later on) and CFM RUN 12-02, where the model calculations achieved a tracer recovery of 100%, were scaled to the recovery of the

ideal tracer, 84%, 90%, and 80%, respectively, to account for the mass losses during the experimental test. For CFM RUN 10-03 due to problems with the uranine tracer a reliable breakthrough curve of an ideal tracer was not available. Only for illustration, the curve for the colloids is shown in Fig. 4, which is also simulated with the same flow parameters, but additional interaction rates for the colloids. The model parameters for flow and transport of the ideal tracer are listed in Tab. 2. The porosity of 0.12 is in the lower range of porosities observed for the fault gauge material from the shear zone but still in agreement with values between 10 and 40% given in [8].

Tab. 2: Geometrical, hydraulic and general parameters

Parameter	Value	Parameter	Value
Dimensionality	2D	Porosity [-]	0.12
Model thickness [m]	$5 \cdot 10^{-3}$	Dispersivity [m] - Longitudinal - Transversal	 0.3 0.1
Dipole distance [m]	6.2	Diffusion coefficient [m^2 s^{-1}]	$2.0 \cdot 10^{-11}$
Temperature [K]	293.15	Permeability [m^2]	$5.5 \cdot 10^{-11}$
Rock density [kg m^3]	2670		

In the second step, after calibrating the flow parameters, the transport of the colloids for CFM RUN 10-01 is simulated. A slight shift of the experimental colloid breakthrough curve indicates a weak retardation of the colloids. A further characteristic is a more smooth increase of the breakthrough curve compared to uranine. The strategy to describe both effects is a kinetically controlled interaction of the colloids with the fracture filling material by the choice of a colloid attachment rate $K_2 = 0.054$ h^{-1} and a detachment rate $k_2 = 0.108$ h^{-1}. This ratio is corresponding to a retardation factor of about 1.5 for the colloids. However, under the conditions considered here, the interaction reaction between colloids and fracture filling material is not in equilibrium. Further, a filtration rate of 0.01 h^{-1} was applied to account for an additional irreversible filtration. The resulting breakthrough curve for the colloids is shown in Fig. 5.

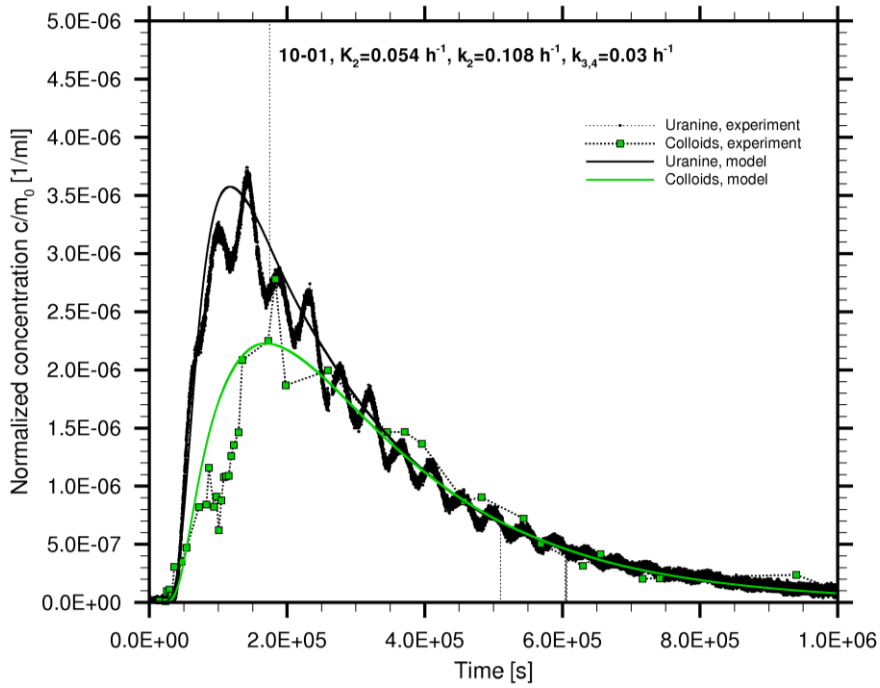

Fig. 5: Experimental and simulated breakthrough curves for CFM RUN 10-01 for the uranine tracer, and the colloids.

In the third step the homologue transport is simulated. Batch sorption experiments suggest that the tri- and tetravalent cations are strongly sorbed onto the fracture filling material, i.e. the non-colloid-bound fraction will not migrate through the dipole during the time the experiment is conducted. Only the colloid-bound fraction is expected to travel at a similar velocity as the fluid.

Therefore, the experiment is determined by the following processes. As described above the homologues are equilibrated with the colloid-bearing solution in advance and are quantitatively bound to the colloids, when injected into the dipole. During the transport through the fracture part of the homologues desorb from the colloids and subsequently adsorb to the fracture filling material. The velocity of these processes is determined by the detachment rate k_3 of the homologues from the colloids, since the adsorption reaction of the homologues to the fracture filling material is assumed to be fast. With an increasing desorption rate k_3 the peak maximum and the recovery of the homologue breakthrough curves decrease.

The experimental curves show a difference between the trivalent and the tetravalent homologues. The peak maximum as well as the recovery is higher for tetravalent thorium and hafnium than for trivalent europium and terbium. Consequently, higher desorption rates are expected for the trivalent homologues. In our model the breakthrough curves are quite well described with a detachment rate $k_{3,4} = 0.03\ h^{-1}$ for the tetravalent and with $k_{3,4} = 0.075\ h^{-1}$ for the trivalent homologues, see Figures 6 and 7.

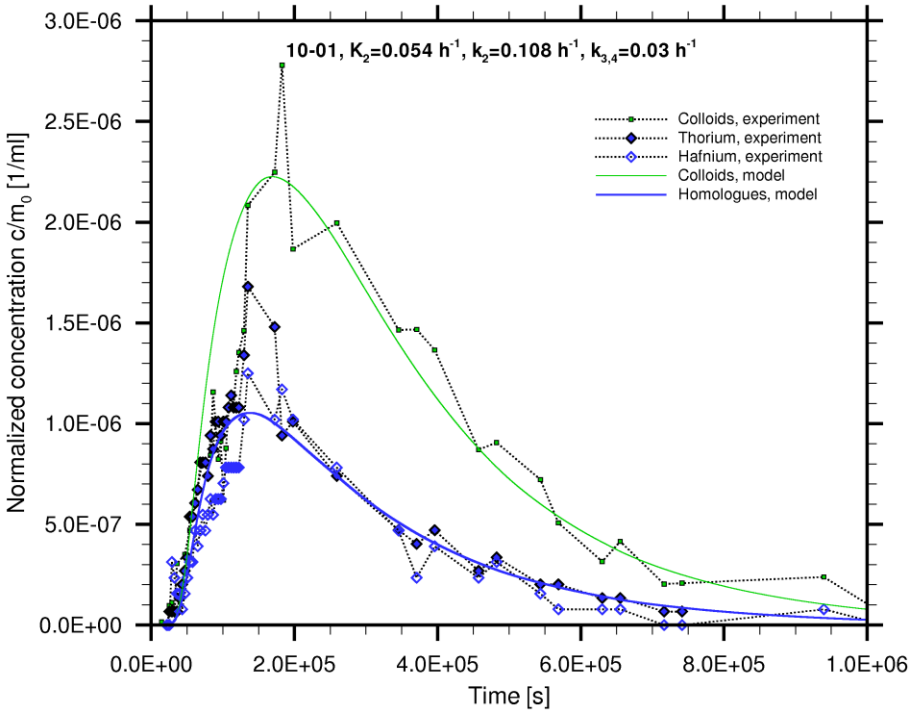

Fig. 6: Simulated and experimental breakthrough curves for the tetravalent homologues hafnium and thorium for CFM RUN 10-01. Best estimate parameter of $k_{3,4}$ are given.

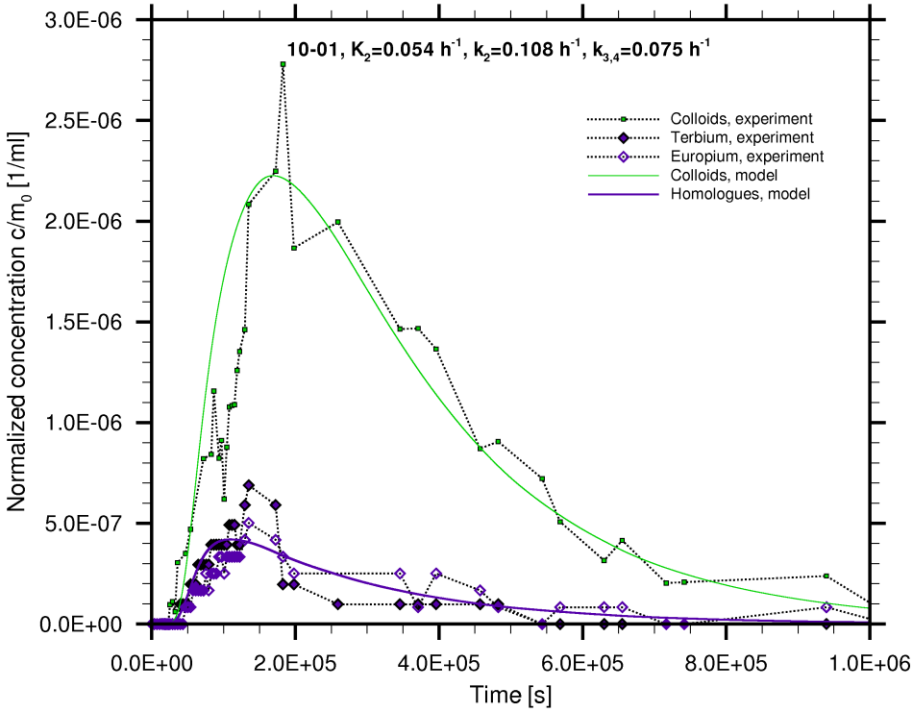

Fig. 7: Simulated and experimental breakthrough curves for the trivalent homologues terbium and europium for CFM RUN 10-01. The best estimate parameter of $k_{3,4}$ is given.

In addition to the shape of the curves the mass recoveries of experiment and simulation can be compared. All these data are listed in Tab. 3. In general, also the recoveries of colloids and homologues in CFM RUN 10-01 are quite well reproduced by the model calculations.
In the same way the colloid and homologue transport for CFM RUN 10-03 is simulated. Due to a lower extraction rate at Pinkel the travel time is increased with respect to CFM RUN 10-01. One important question is, whether the breakthrough curves and recoveries can be described with the same interaction rates. For the colloids the same interaction parameters as applied for CFM RUN 10-01 gives a reasonable result with respect to the peak of the breakthrough curve. However, the tailing at travel times >400 h is slightly underestimated. Nevertheless, the recovery of 41% observed in the experiment is again well reproduced by the calculation with a value of 45.1% (Tab. 3).

For the homologues it became clear that significantly lower desorption rates have to be assumed than those for CFM RUN 10-01. This is already apparent, when looking at the recoveries, which are similar for both tests, in case of tetravalent homologues even higher in CFM RUN 10-03 than in CFM RUN 10-01. This is unexpected, since a longer travel time should increase the amount of desorbed homologues and therewith lead to a reduced recovery. Therefore, for CFM RUN 10-03 lower desorption rates of 0.02 h^{-1} and 0.0025 h^{-1} have been applied to describe the breakthrough curves of the tri- and tetravalent homologues, respectively. With these rates the peak of the curves are well reproduced but again the tailing and also the recoveries are to some extent underestimated.

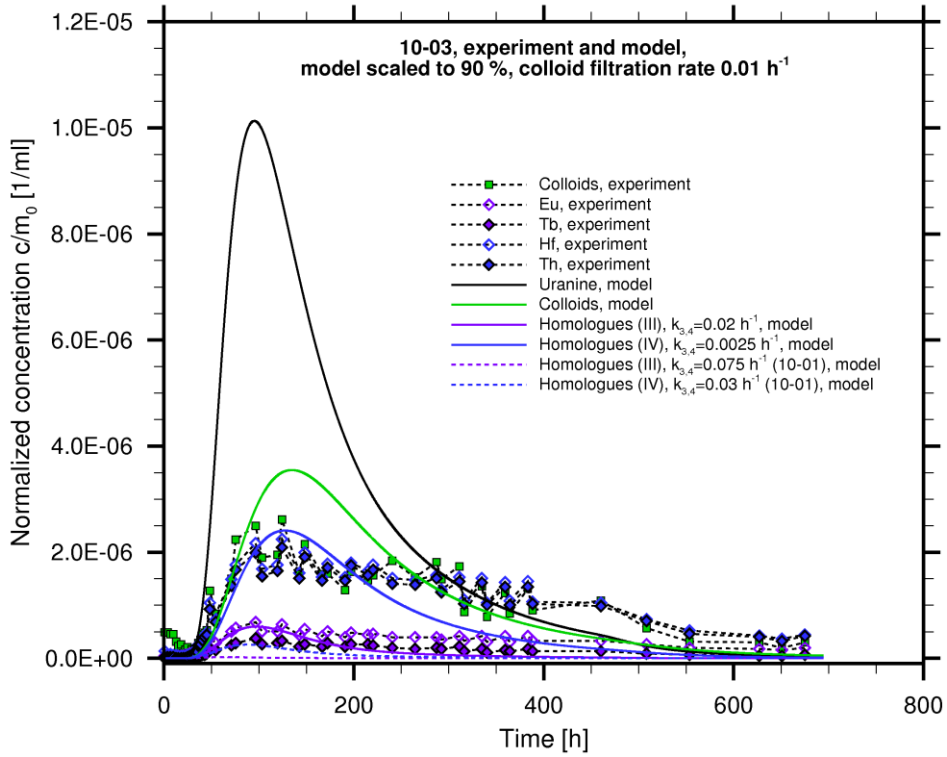

Fig. 8: Simulated and experimental breakthrough curves for the colloids as well as for the trivalent and tetravalent homologues europium, terbium, hafnium and thorium for CFM RUN 10-03. The best estimate parameters of $k_{3,4}$ are given.

Tab. 3: Mass recoveries [%] for CFM RUNs 10-01, 10-03 and for the model simulations

	CFM RUN 10-01		CFM RUN 10-03	
	experiment	model	experiment	model
Colloids	64 53 47	67.2	41	45.1
Homologues (IV)	Th: 32 Hf: 30	27.7	Th: 43 Hf: 46	27.7
Homologues (III)	Tb: 7 Eu: 14	9.9	Tb: 6 Eu: 14	4.9

Sorption data for the homologues and particularly the desorption rates from the colloids have been determined by independent batch experiments for the ternary system homologue – colloid – fracture filling material [13]. In these experiments the pollutants are equilibrated with colloids in solution for a view days before adding the fracture filling materials. After addition of the fracture filling material part of the pollutants desorb from the colloids and sorb on the fracture filling material. Assuming that the time dependence of the K_d-value is determined by the desorption rate, that the process is in equilibrium after 7500 h (the endpoint of the experiment) and neglecting an interaction of the colloid with the fracture filling material *Huber et al.* derived detachment rates from the colloids of 0.0037 h^{-1} for americium and 0.0014 h^{-1} for the tetravalent elements plutonium and thorium [13]. A batch modeling attempt using the same sorption coefficients and attachment rates as applied for the field experiment for Am and Pu yielded similar detachment rates k_3/k_4 of 0.0035 h^{-1} and 0.0022 h^{-1} for Am and Pu, respectively. The resulting curves compared to the experimental data are shown in Fig. 9.

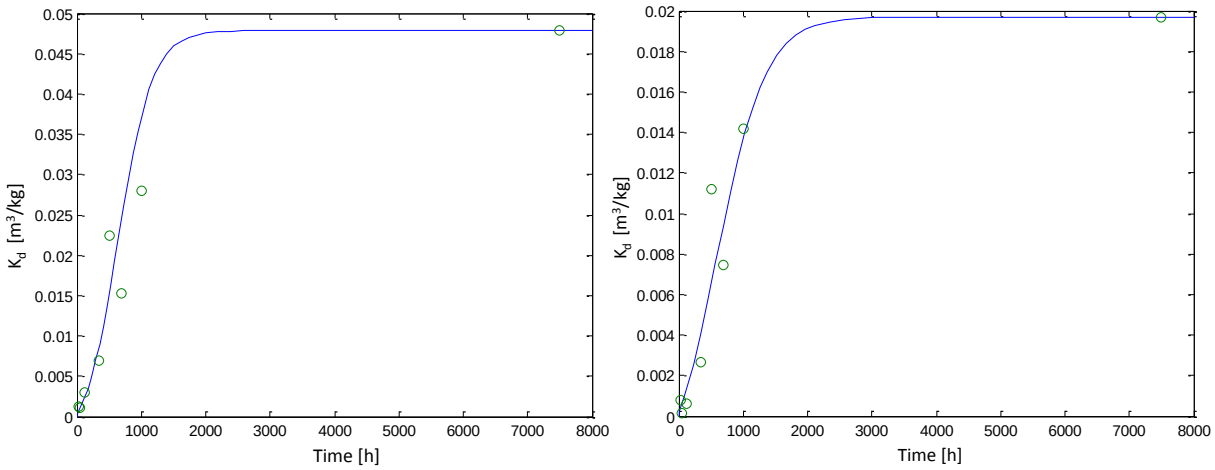

Fig. 9: K_d-values for experiment (dots, [11]) and simulation (line) as a function of time in the ternary batch system bentonite colloids, fracture infill and pollutant Am (left, model data: K_{d1} = 2 m^3/kg, K_{d3} = 1600 m^3/kg, k_1= 1 h^{-1} and k_3 = 0.0035 h^{-1}) and Pu (right, model data: K_{d1} = 0.825 m^3/kg, K_{d3} = 1600 m^3/kg, k_1= 1 h^{-1} and k_3 = 0.0022 h^{-1}).

The results show, that the desorption rates, which are determining the homologue breakthrough curves and recoveries, derived in our model simulations for CFM RUN 10-03 are in a similar range as those derived from independent batch experiments. For CFM RUN 10-01 performed at higher extraction rate and therewith lower residence time higher desorption rates are observed. Such decrease in reaction rates is observed in other natural systems and was also found for the transport of lanthanides bound to humics, e.g. [12]. However, the reason for this difference in desorption rates in experiments discussed here is not yet clear. One explanation might be that the colloid concentration in CFM RUN 10-03 is significantly higher, whereas the concentration of homologues is the same. Therefore, a decreased desorption rate of homologues at lower coverage of the bentonite colloids could explain this behavior. But, so far, there is no experimental evidence for this.

Concerning the interaction of colloids with the fracture filling material the filtration (attachment) rate K_2 can be compared to results from deep bed filtration theory. The common approach of the deep bed filtration, neglecting the detachment of filtered colloids leads to

$$K_2\Theta = \lambda_f q_C \qquad \text{(Eq. 6)}$$

The particle velocity is denoted as q_C. The efficiency of the filtration can be described by the filter coefficient λ_f. Here it is assumed that the mechanism is independent of the amount of already filtrated colloids as it is for clean deep bed filtration. Important parameters are the porosity and pore size of the sediment, the diameter of the colloidal particles, and the viscosity. Here we refer to the model of *Tien and Payatakes* [14]. Under the conditions of the field experiment, particularly for an average colloid size in the range of 150 nm [15], the filtration efficiency η is dominated by diffusion and can be calculated according to *Yao et al.* [16] neglecting interception and sedimentation processes by

$$\eta_D = 0.9\left(\frac{k_B T}{\mu d_p d_C q_C}\right)^{2/3} \qquad \text{(Eq. 7)}$$

with the Boltzmann constant k_B, the Temperature T, the viscosity μ, the particle diameter d_p and the collector diameter d_c.

The filter coefficient is then defined as

$$\lambda_f = \frac{3}{2}\frac{1-\Theta}{d_C}\eta\alpha \qquad \text{(Eq. 8)}$$

The attachment factor α describes the part of the colloid-matrix collisions which lead to binding. The attachment process of colloidal bentonite particles on granite infill material under Grimsel conditions has been investigated in experiments by *Degueldre et al.* [17]. From these investigations an attachment factor of $2 \cdot 10^{-4}$ was determined. All other

parameters, which are adapted to the conditions of the CFM experiments, are listed in Tab. 4. The viscosity and fluid density are given for the low mineralized Grimsel groundwater. For the bentonite colloids the rock density of bentonite is applied. A collector diameter of 10^{-4} m is selected as an average grain size of the fracture infill material. For the particle velocities in the range of 10^{-4} to 10^{-5} m/s filtration rates K_2 = 0.11 to 0.05 h^{-1} are calculated, which are higher than the irreversible rate of 0.01 h^{-1}. However, taking into account that we have assumed an additional reversible attachment process, with a rate of 0.054 h^{-1}, the observed interaction rates fit into the range obtained by deep bed filtration theory.

Tab. 4 Parameters used for the deep bed filtration approach

Parameter	**unit**	**Value**
dynamic viscosity μ	Ns/m^2	$1 \cdot 10^{-3}$
fluid density ρ	kg/m^3	1000
colloid density ρ_P	kg/m^3	2670
collector diameter d_C	m	$1 \cdot 10^{-4}$
gravitation constant g	m/s^2	9.81
temperature T	K	288.15
Boltzmann constant k_B	J/K	$1.38 \cdot 10^{-23}$
porosity Θ		0.15
attachment factor α		$2 \cdot 10^{-4}$

5 CONCLUSIONS

Selected field experiments performed in a shear zone at the Grimsel Test Site within the international Colloid Formation and Migration (CFM) project have been simulated with a 2D numerical model. Although the transport pathway in the shear zone is described as a porous medium using effective parameters, the flow of the ideal tracers can be well described with one set of parameters for flow conditions varying over one order of magnitude with respect to the fluid travel time.

Transport simulations have been performed for two field dipole experiments with colloids and tri- and tetravalent homologues, varying in the extraction rate between 48 ml/min (CFM RUN 10-01) and 10 ml/min (CFM RUN 10-03). The colloid-facilitated transport is described by kinetically controlled interactions between the homologues, the colloids and the surface of the fracture filling material. The interaction of the colloids with the fracture filling material can be reasonably well described by one set of parameters for both experiments considering a reversible and an irreversible attachment process. Attachment rates obtained from deep bed filtration theory are in the same order of magnitude as those derived from simulation of the experiments.

For the interaction of the homologues with the colloids the desorption process of the homologues from the colloids is most relevant. It determines the shape of the breakthrough curve and the recovery of the homologues. The desorption rates obtained from the field experiment at longer residence time agree homologues, particularly for the tetravalent, well with desorption rates derived from independent batch experiments in ternary systems. The desorption rates at lower residence times are significantly higher. The reason for this difference is not yet clear and will be further investigated in additional migration experiments at different dipoles in the shear zone, which are intended to be performed in the near future.

6 ACKNOWLEDGEMENT

This work was financed by the German Federal Ministry of Economics and Technology (BMWi) under contract no. 02 E 10669 and 02 E 10679 in the framework of the KOLLORADO-2 project. We also would like to thank the partners from the CFM project at Grimsel Test Site - KIT-INE (Germany), JAEA (Japan), SKB (Sweden), CRIEPI (Japan), KAERI (Republic of Korea), POSIVA (Finland), NAGRA (Switzerland), USDOE (USA).

7 REFERENCES

1. Missana, T., Alonso, T., Turrero, M.J.S. (2003): Generation and stability of bentonite colloids at the bentonite/granite interface of a deep geological radioactive waste repository. Journal of Contaminant Hydrology, 61(1-4), p. 17-31.
2. Alonso, U., Missana, T., Geckeis, H., Garcia-Gutierrez, M., Turrero, M.J., Möri, R., Schäfer, T., Patelli, A., Rigato V. (2006): Role of inorganic colloids generated in a high-level deep geological repository in the migration of radionuclides: open questions. Journal of Iberian Geology, 32(1), p. 79.
3. Baik, M.H., Cho, W.J., Hahn, P.S. (2007): Erosion of bentonite particles at the interface of a compacted bentonite and a fractured granite. Engineering Geology, 91(2-4), p. 229-239.
4. Schäfer, T., Huber, F., Seher, H., Missana, T., Alonso, U., Kumke, M., Eidner, S., Claret, F., and Enzmann, F. (2012): Nanoparticles and their influence on radionuclide mobility in deep geological formations. Appl. Geochem. 27, 390-403.
5. SKB (2011): Long-term safety for the final repository for spent nuclear fuel at Forsmark. Main report of the SR-Site project. Volume I – III. Svensk Kärnbränslehantering AB, March 2011.
6. Blechschmidt, I. and Lanyon, B. (2008): GTS Phase VI, CFM Phase 1, Field Activities 2006 – 2008. NAGRA Arbeitsbericht NAB 08-33,NAGRA: Wettingen (Switzerland). p.69.
7. Geckeis, H., Rabung, T., and Schäfer, T. (2011): Actinide - Nanoparticle interaction: generation, stability and mobility. In: Kalmykov, S. N. and Denecke, M. A. (Eds.), Actinide Nanoparticle Research. Springer-Verlag, Berlin, Heidelberg.
8. Gaus, I., Smith, P.A. (2008): Modellers dataset for the Colloid Formation and Migration Project Status: End of CFM Phase 1. NAGRA Arbeitsbericht NAB 08-27, NAGRA: Wettingen (Switzerland).
9. Fein, E., Schneider, A. (1999): Ein Programmpaket zur Modellierung von Dichteströmungen. Gesellschaft für Anlagen- und Reaktorsicherheit (GRS) mbH, GRS-139, Braunschweig, Germany.
10. Fein, E. (ed.) (2004): Software package r^3t – Model for transport and retention in porous media. Final report. Gesellschaft für Anlagen- und Reaktorsicherheit (GRS) mbH, GRS-192, Braunschweig, Germany.
11. Flügge, J., Küntzel, M., Schäfer, T., Gaus, I., Noseck, U. (2010): Modeling colloid-bound radionuclide transport at the Grimsel test site. In: “Proceedings of the International Groundwater Symposium by IAHR”, Valencia, Spain, September 22-24, 2010.
12. Lührmann, L.; Noseck, U.; Tix C. (1998): Model of contaminant transport in porous media in the presence of colloids applied to actinide migration in column experiments. Water Resources Research, **34**(3), p. 421-426.
13. Huber, F., Kunze, P., Geckeis H., Schäfer T. (2011): Sorption reversibility kinetics in the ternary system radionuclide - bentonite colloids/nanoparticles - granite fracture filling material. Appl. Geochem. **26**(12), p. 2226-2237.

14. Tien, C., Payatakes, A.C. (1979): Advances in deep bed filtration. Am. Inst. Chem. Eng., AIChE, **25**(5), p. 737.

15. Schäfer, T, Noseck, U, (eds.) (2010): Colloid/ Nanoparticle formation and mobility in the context of deep geological nuclear waste disposal (Project KOLLORADO; Final report). FZKA report 7515, Institut für Nukleare Entsorgung: Karlsruhe, Gesellschaft für Anlagen- und Reaktorsicherheit (GRS) mbH, Braunschweig.

16. Yao, K.M., Habibian, M.T., O'Melia, C.R. (1971): Water and Wastewater Filtration: Concepts and Applications. Environmental Science and Technology, **5**, p. 1105-1112.

17. Degueldre, C., Grauer, R., Laube, A., Oess, A., Silby, H. (1996): Colloid properties in granitic groundwater systems. 2. Stability and transport study. Applied Geochemistry, **11**(5), p. 697.